

## Epitaxial $\text{Pb}(\text{Zr}_{0.52}\text{Ti}_{0.48})\text{O}_3/\text{La}_{0.35}\text{Nd}_{0.35}\text{Sr}_{0.3}\text{MnO}_3$ heterostructures for fabrication of ferroelectric field-effect transistor

Wenbin Wu, K. H. Wong, C. L. Mak, C. L. Choy, and Y. H. Zhang

Citation: *J. Appl. Phys.* **88**, 2068 (2000); doi: 10.1063/1.1305859

View online: <http://dx.doi.org/10.1063/1.1305859>

View Table of Contents: <http://jap.aip.org/resource/1/JAPIAU/v88/i4>

Published by the [American Institute of Physics](#).

---

### Related Articles

Surface rippling on bulk metallic glass under nanosecond pulse laser ablation

*Appl. Phys. Lett.* **99**, 191902 (2011)

Negative ions: The overlooked species in thin film growth by pulsed laser deposition

*Appl. Phys. Lett.* **99**, 191501 (2011)

High-frequency electromagnetic properties of epitaxial  $\text{Bi}_2\text{FeCrO}_6$  thin films grown by pulsed laser deposition

*Appl. Phys. Lett.* **99**, 183505 (2011)

Al and Fe co-doped transparent conducting ZnO thin film for mediator-less biosensing application

*AIP Advances* **1**, 042112 (2011)

Effects of stress on the optical properties of epitaxial Nd-doped  $\text{Sr}_{0.5}\text{Ba}_{0.5}\text{Nb}_2\text{O}_6$  films

*AIP Advances* **1**, 032172 (2011)

---

### Additional information on J. Appl. Phys.

Journal Homepage: <http://jap.aip.org/>

Journal Information: [http://jap.aip.org/about/about\\_the\\_journal](http://jap.aip.org/about/about_the_journal)

Top downloads: [http://jap.aip.org/features/most\\_downloaded](http://jap.aip.org/features/most_downloaded)

Information for Authors: <http://jap.aip.org/authors>

### ADVERTISEMENT

**AIP**Advances

*Submit Now*

Explore AIP's new  
open-access journal

- Article-level metrics now available
- Join the conversation! Rate & comment on articles

# Epitaxial $\text{Pb}(\text{Zr}_{0.52}\text{Ti}_{0.48})\text{O}_3/\text{La}_{0.35}\text{Nd}_{0.35}\text{Sr}_{0.3}\text{MnO}_3$ heterostructures for fabrication of ferroelectric field-effect transistor

Wenbin Wu<sup>a)</sup>

Structure Research Laboratory, University of Science and Technology of China, Hefei 230026, China  
and Department of Applied Physics, The Hong Kong Polytechnic University, Kowloon, Hong Kong, China

K. H. Wong, C. L. Mak, and C. L. Choy

Department of Applied Physics, The Hong Kong Polytechnic University, Kowloon, Hong Kong, China

Y. H. Zhang

Structure Research Laboratory, University of Sciences and Technology of China, Hefei 230026, China

(Received 11 February 2000; accepted for publication 9 May 2000)

Epitaxial  $\text{La}_{0.35}\text{Nd}_{0.35}\text{Sr}_{0.3}\text{MnO}_3$  (LNSMO) thin films and  $\text{Pb}(\text{Zr}_{0.52}\text{Ti}_{0.48})\text{O}_3$  (PZT)/LNSMO heterostructures have been grown on  $\text{LaAlO}_3$  (001) substrates by the pulsed laser deposition method. The oxygen concentration in the LNSMO films is quite sensitive to the deposition oxygen pressure and can be controlled during the fabrication process. It is, however, stable against *in situ* postdeposition thermal treatments. Consequently, the resistivity and the metal-semiconductor transition temperature of the LNSMO films can be tuned and fixed during film growth. Electrical measurements on the Pt/PZT/LNSMO ferroelectric capacitor show a remnant polarization of  $\sim 35 \mu\text{C}/\text{cm}^2$  and a coercive field of 30–40 kV/cm at low driving voltages. Switching endurance tests suggest no polarization loss up to about  $10^{10}$  bipolar switching cycles. The advantages of using epitaxial LNSMO films as the semiconducting channel in an all-perovskite ferroelectric field-effect transistor are discussed. © 2000 American Institute of Physics. [S0021-8979(00)04616-8]

## I. INTRODUCTION

The ferroelectric field-effect transistor (FeFET), which uses a ferroelectric thin film as the gate insulator, is expected to possess fast write/erase and read-access speeds as well as nonvolatility. Over the past few years, several groups have proposed novel FeFET devices based on the use of all-perovskite ferroelectric/semiconductor heteroepitaxial structures.<sup>1,2</sup> An example of such FeFET consists of a ferroelectric  $(\text{Pb},\text{La})(\text{Zr},\text{Ti})\text{O}_3$  gate and a  $\text{Sr}_{1-x}\text{CuO}_2$  or  $\text{La}_{1.99}\text{Sr}_{0.01}\text{CuO}_4$  semiconductor channel. In comparison with the more conventional FeFET having Si as the semiconducting channel layer, a markedly improved ferroelectric field effect has been observed. This is attributed to the well-controlled and high quality interface between the epitaxial gate and the channel layers in the all-perovskite structures. Recently, the doped manganates exhibiting colossal magnetoresistance have also been used as the semiconductor channel materials for FeFETs. A modulation in channel resistance of at least a factor of 3 and a retention on the order of hours have been achieved.<sup>3</sup> These manganates are perovskites and are closely lattice matched to the common perovskite ferroelectrics. They show a metal-semiconductor transition near the Curie temperature. Their electrical resistivity and transition temperature, however, change with carrier concentration which varies widely with both the cation doping level and oxygen stoichiometry.<sup>4–6</sup> Moreover, with the use of manganate films as the semiconducting channel, the field-effect device may potentially be both electrically and magnetically tuned.

Grishin, Khartsev, and Johnsson have demonstrated the coexisting magnetoresistive and ferroelectric properties in epitaxial  $\text{Pb}(\text{Zr}_{0.52}\text{Ti}_{0.48})\text{O}_3$  (PZT)/manganate heterostructures.<sup>7</sup> As has been pointed out, in order to obtain a large modulation in the channel resistance, the number of carriers in the channel layer needs to be tuned with respect to the amount of available charge induced by the ferroelectric gate.<sup>3,8</sup> In this work, epitaxial  $\text{La}_{0.33}\text{Nd}_{0.35}\text{Sr}_{0.3}\text{MnO}_3$  (LNSMO) films and PZT/LNSMO heterostructures have been fabricated by pulsed laser deposition method. We show that the oxygen concentration in the LNSMO layers can be controlled during the *in situ* fabrication process. The oxygen stoichiometry of the LNSMO films is quite sensitive to the ambient oxygen pressure during deposition. It is nevertheless, highly stable against *in situ* postdeposition annealing at various oxygen pressures. High quality epitaxial ferroelectric PZT films grown on the LNSMO layers of different oxygen contents have been obtained.

## II. EXPERIMENT

LNSMO films and PZT/LNSMO heterostructures were grown on  $\text{LaAlO}_3$ (001) (LAO) substrates by *in situ* pulsed laser deposition using a KrF 248 nm excimer laser with a repetition rate of 10 Hz. The laser energy density irradiated on the rotating LNSMO and PZT targets was 6 and 3 J/cm<sup>2</sup>, respectively. The target–substrate distance was 50 mm. The chamber was evacuated by a cryopump to a base pressure of  $5 \times 10^{-7}$  Torr. For the LNSMO films, the deposition and *in situ* annealing temperature was fixed at 700 °C. The oxygen pressure during deposition was varied in the range of 300–10 mTorr. Some of the films were *in situ* annealed at

<sup>a)</sup>Electronic mail: wuwb@ustc.edu.cn

oxygen pressure ranging from  $2 \times 10^{-6}$  to 760 Torr for up to 2 h. They were then cooled to room temperature in the same annealing atmosphere. For the PZT/LNSMO heterostructures, the LNSMO layers were first grown at 700 °C in oxygen pressure of 100, 60, and 25 mTorr, respectively. PZT films were deposited *in situ* on top at 620 °C in an oxygen ambient of 250 mTorr. The as-grown heterostructures were cooled under 1 atm of oxygen pressure. The thickness of the LNSMO and PZT films is measured to be about 100 and 500 nm, respectively. The deposition rate for the LNSMO films is calibrated to be 10–15 nm/min and it decreases with the deposition oxygen pressure.

The crystal structure of the LNSMO films and the PZT/LNSMO heterostructures was characterized using a four-circle x-ray diffractometer with Cu  $K\alpha$  radiation. The electrical transport properties were examined by resistance–temperature ( $R$ – $T$ ) measurements of a standard four-point method. In order to form capacitive cells, circular Pt electrodes ( $\varnothing=0.2$  mm) were sputtered through a contact mask on the top of the PZT layer at room temperature. The ferroelectric properties of the heterostructures were measured by a RT66A standardized test system. The polarization fatigue tests were performed using square wave of  $\pm 6$  V at 25 kHz.

### III. RESULTS AND DISCUSSION

Figure 1(a) shows the  $R$ – $T$  curves of the LNSMO films deposited under different oxygen pressure. The as-grown films were cooled to room temperature at their corresponding deposition ambient. No postannealing was carried out on these samples. It is seen that the metal–semiconductor transition temperature,  $T_p$ , of these films decreases with the deposition pressure. The overall resistivity of the films, on the other hand, gets progressively larger at lower growth pressure. Magnetization versus temperature measurements indicate that the  $T_p$  is consistent with the magnetic transition temperature,  $T_C$ , for each of the samples. The x-ray diffraction (XRD) measurements reveal that the films deposited at different oxygen pressures are all cube-on-cube grown on the LAO(001) substrates. In the inset to Fig. 1(a), an almost linear relationship between the out-of-plane lattice constant,  $d$ , and  $T_p$  of the LNSMO films is obtained. These observations are similar to those reported for the  $\text{La}_{0.7}\text{Ca}_{0.3}\text{MnO}_3$  system.<sup>6</sup>

Although the manganate films are very sensitive to the deposition oxygen pressure, their response to the oxygen background during the *in situ* annealing process is quite different. In order to study the thermal stability of the LNSMO films, the as-grown films deposited at the same oxygen ambient were immediately *in situ* annealed at different oxygen pressures. Over 20 samples were studied and the results are highly reproducible. A typical set of results is shown in Fig. 1(b), where the LNSMO films deposited at 300 mTorr were *in situ* annealed at  $2 \times 10^{-6}$  and 10 Torr, respectively. It is seen that the LNSMO films show almost the same electrical transport behavior. Apparently the oxygen content of the as-deposited films has not been changed during the *in situ* annealing process. This is also reflected by the XRD data for films that have undergone a different annealing process. For

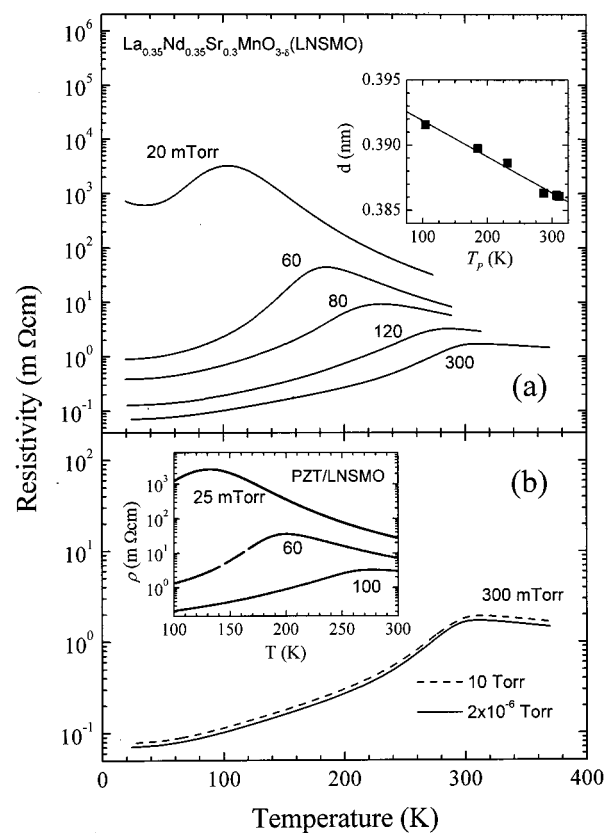


FIG. 1. (a)  $R$ – $T$  curves of epitaxial LNSMO films deposited under an oxygen pressure of 300, 120, 80, 60 and 20 mTorr, as denoted. The inset shows the relationship between the out-of-plane lattice constant,  $d$ , and  $T_p$  of the LNSMO films. (b)  $R$ – $T$  curves of epitaxial LNSMO films grown at 300 mTorr and then *in situ* annealed at 10 (dashed line) and  $2 \times 10^{-6}$  Torr (solid line) of oxygen pressure, respectively. The inset shows  $R$ – $T$  curves for the LNSMO layer in epitaxial PZT/LNSMO heterostructures with the LNSMO deposited at 100, 60 and 25 mTorr, as denoted.

the two films annealed at  $2 \times 10^{-6}$  and 10 Torr ambient oxygen, the peaks of the LNSMO(002) reflections remain at the same position (not shown). This observed high thermal stability distinguishes the LNSMO films from many other perovskite-type conductive films such as  $\text{La}_{0.5}\text{Sr}_{0.5}\text{CoO}_3$ .<sup>9</sup> Our results also indicate that the *in situ* annealing effect on the manganate films is quite different from the *ex situ* annealing effects reported previously.<sup>10</sup>

Figure 2 shows the XRD results on a typical PZT/LNSMO heterostructure with the LNSMO layer deposited at 25 mTorr. The patterns shown in Figs. 2(a) and 2(b) are linear scans along the normal of LAO(001) (specular) and LAO(101) (off-specular) diffraction planes of the same heterostructure. From the two scans, it may be concluded that a parallel epitaxial growth of the heterostructure on the substrate has been achieved. The insets to Figs. 2(a) and 2(b) are  $\omega$ -scan rocking curves on PZT(002), LNSMO(002), and LAO(002) reflections, and  $\phi$  scans on PZT(101) and LAO(101) reflections, respectively. These curves further suggest that the heterostructure has good crystallinity and epitaxial properties. Note that the off-specular linear ( $\theta$ – $2\theta$ ) scan shown in Fig. 2(b) was recorded by setting the  $\phi$  angle at one of the four peak positions corresponding to the LAO(101)  $\phi$  scan shown in the inset to Fig. 2(b), and the  $\chi$

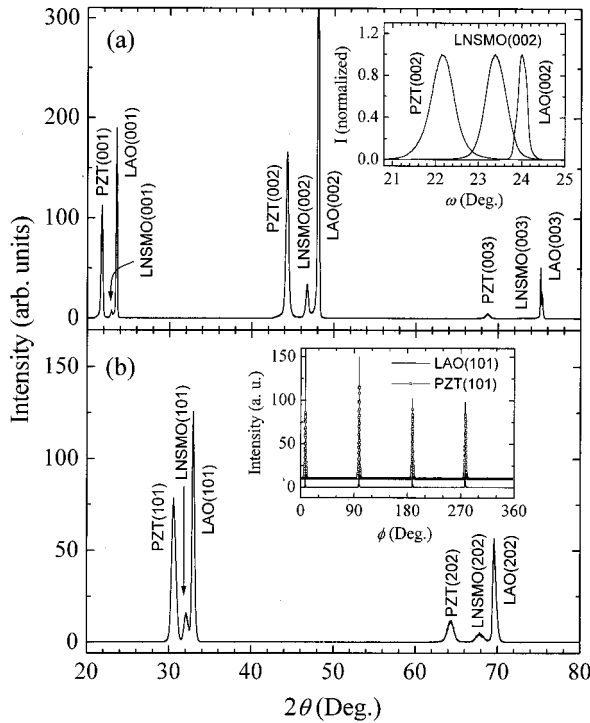


FIG. 2. XRD specular (a) and off-specular (b) linear scans from a PZT/LNSMO/LAO(001) heterostructure with the LNSMO layer deposited at 25 mTorr of O<sub>2</sub> ambient. The profile in (b) was measured with the  $\phi$  angle at 94.6° and the  $\chi$  angle at 45°. The insets in (a) and (b) show  $\omega$ -scan rocking curves on the PZT(002), LNSMO(002), and LAO(002) reflections, and  $\phi$  scans on the PZT(101) and LAO(101) reflections, respectively.

angle at 45° due to the pseudocubic structure of the LAO substrates.

Figure 3 shows XRD specular linear scans of the PZT/LNSMO heterostructures with the LNSMO grown at 100 and 60 mTorr, respectively. Although the epitaxial growth of PZT was performed at a higher oxygen pressure and the heterostructures were cooled under an oxygen pressure of 1 atm, the oxygen contents in the LNSMO layers remain fixed,

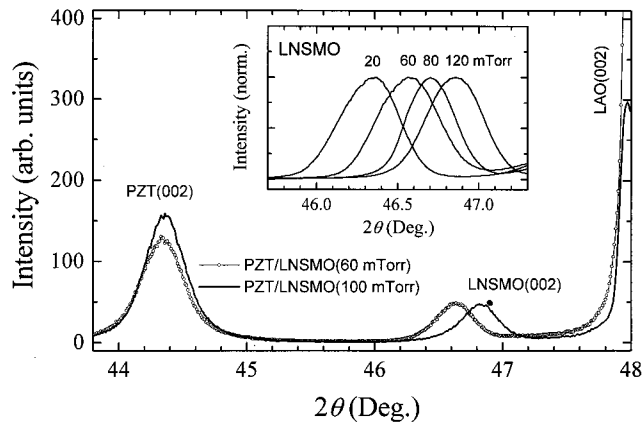


FIG. 3. XRD specular linear scans from the PZT/LNSMO/LAO(001) heterostructures. The PZT layer was deposited at 250 mTorr and the LNSMO layer was deposited at oxygen ambient of 100 or 60 mTorr, respectively. The inset shows XRD linear scans around the LNSMO(002) peak positions of the LNSMO films grown at various oxygen pressures.

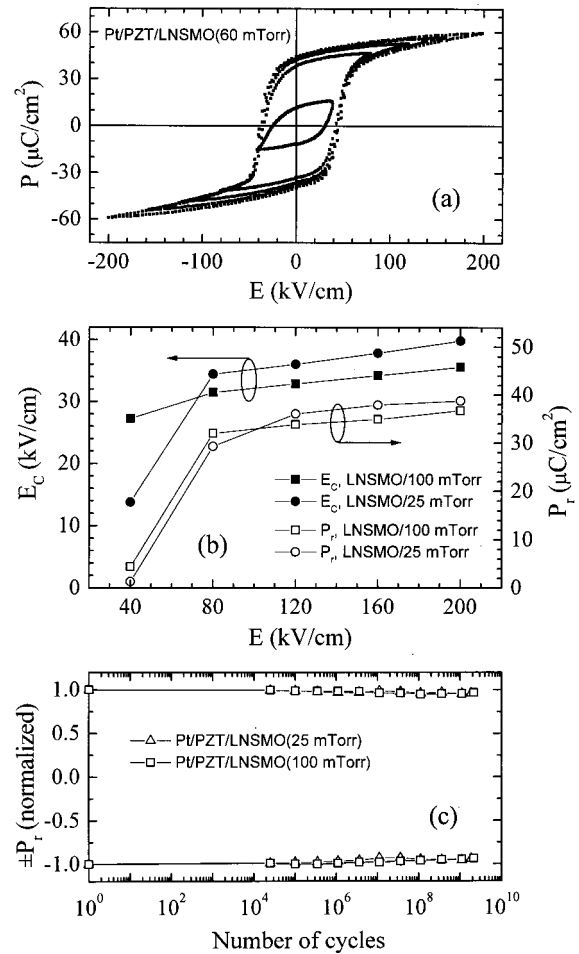


FIG. 4. (a) Typical  $P$ - $E$  hysteresis loops for the PZT film on the LNSMO deposited at 60 mTorr of O<sub>2</sub> ambient. The data were taken at the maximum driving voltages of 2, 4, 6, 8 and 10 V. (b) Field dependence of the  $P_r$  and  $E_c$  of the PZT films on LNSMO deposited at various oxygen pressures. (c) Fatigue properties of the Pt/PZT/LNSMO capacitors, tested with peak voltage of  $\pm 6$  V at 25 kHz.

as shown by the PZT(002) and LNSMO(002) peak positions. For comparison, in the inset to Fig. 3, LNSMO(002) reflections from the LNSMO films shown in Fig. 1(a) are also presented. The tunability and stability of the oxygen content in the channel layer is also demonstrated by the  $R$ - $T$  measurements of the LNSMO in the heterostructures, where the LNSMO layers were deposited at 100, 60, and 25 mTorr, respectively. The inset to Fig. 1(b) shows that the  $T_p$  and the overall resistivity of the LNSMO channels in the heterostructures are almost the same as those recorded for the LNSMO single layer films deposited at similar oxygen pressures.

Ferroelectric hysteresis and switching fatigue have also been measured for the PZT/LNSMO heterostructures. The LNSMO layers were grown at various deposition oxygen pressures. Figure 4(a) shows some typical polarization versus electrical-field ( $P$ - $E$ ) loops recorded for a Pt/PZT/LNSMO capacitor with the LNSMO film grown at 60 mTorr. The five loops represent the maximum driving voltages of 2, 4, 6, 8, and 10 V. The loops are quite square and symmetrical. The remnant polarization ( $P_r$ ) is almost saturated at 4 V with  $P_r = 35 \mu\text{C}/\text{cm}^2$  and coercivity  $E_c = 34$

kV/cm. Figure 4(b) shows the  $P_r$  and  $E_c$  measured from the PZT films on LNSMO layers deposited at 100 and 25 mTorr. The two PZT films have comparable  $P_r$  and the film on the LNSMO layer grown at 25 mTorr shows a higher  $E_c$ . This may simply be ascribed to the effect due to lower conductivity of the LNSMO electrode. To further characterize the ferroelectric properties of the PZT films, polarization switching fatigue tests were performed and the results are shown in Fig. 4(c). Although Pt was used as the top electrodes, the capacitors show no sign of loss of polarization after  $10^9$  cycles, indicating that the manganate films are a more suitable electrode material for ferroelectric capacitors than many other electrical conductive perovskites.<sup>11,12</sup> This improved polarization fatigue behavior could be interpreted in terms of the high thermal stability of the LNSMO bottom electrodes. Due to the high thermal stability, defects at the PZT/LNSMO interface may be greatly reduced during the fabrication process. The above-mentioned results thus suggest that the manganates are desirable materials for fabrication of fatigue-free all-perovskite FeFET.

#### IV. CONCLUSIONS

In summary, epitaxial PZT/LNSMO heterostructures for FeFETs have been grown on LAO substrates by the pulsed laser deposition method. Oxygen content in the LNSMO channel layer can be properly tuned by *in situ* controlling the deposition oxygen pressure. High thermal stability of the LNSMO films has been demonstrated. Oxygen concentration and hence the electrical transport properties of the channel layer is well preserved during the subsequent deposition of the ferroelectric gate. Due to the high thermal stability and the close lattice matching of the constituent layers, the Pt/

PZT/LNSMO heterostructures exhibit excellent structural and electrical properties. A large  $P_r=35 \mu\text{C}/\text{cm}^2$  and a low  $E_c=34 \text{ kV}/\text{cm}$  at low driving voltage of 4 V are obtained. No apparent loss of polarization for bipolar switching up to  $10^{10}$  cycles has been observed. Our results strongly suggest that the manganates are desirable materials for fabrication of fatigue-free all-perovskite FeFET.

#### ACKNOWLEDGMENTS

This work was supported by the Research Grants Council of the Hong Kong Special Administrative Region under Project No. PolyU5160/98P, and the Chinese Natural Science Foundation.

<sup>1</sup>Y. Watanabe, Appl. Phys. Lett. **66**, 1770 (1995).

<sup>2</sup>C. H. Ahn, J.-M. Triscone, N. Archibald, M. Decroux, R. H. Hammond, T. H. Geballe, Ø. Fischer, and M. R. Beasley, Science **269**, 373 (1995).

<sup>3</sup>S. Matthews, R. Ramesh, T. Venkatesan, and J. Benedetto, Science **276**, 238 (1997).

<sup>4</sup>H. Y. Hwang, S.-W. Cheong, P. G. Radaelli, M. Marezio, and B. Batlogg, Phys. Rev. Lett. **75**, 914 (1995).

<sup>5</sup>J. Fontcuberta, B. Martinez, A. Seffar, S. Pinol, J. L. Carcia-Munoz, and X. Obradors, Phys. Rev. Lett. **76**, 1122 (1996).

<sup>6</sup>A. Goyal, M. Rajeswari, R. Shreekala, S. E. Lofland, S. M. Bhagat, T. Boettcher, C. Kwon, R. Ramesh, and T. Venkatesan, Appl. Phys. Lett. **71**, 2535 (1997).

<sup>7</sup>A. M. Grishin, S. I. Khartsev, and P. Johnson, Appl. Phys. Lett. **74**, 1015 (1999).

<sup>8</sup>C. H. Ahn *et al.*, Appl. Phys. Lett. **70**, 206 (1997).

<sup>9</sup>S. Madhukar, S. Aggarwal, A. M. Dhote, R. Ramesh, A. Krishnan, D. Keeble, and E. Poindexter, J. Appl. Phys. **81**, 3543 (1997).

<sup>10</sup>H. L. Ju and K. M. Krishnan, Solid State Commun. **104**, 419 (1997).

<sup>11</sup>R. Ramesh, W. K. Chan, B. Wilkens, H. Gilchrist, T. Sands, J. M. Tarascon, D. K. Fork, J. Lee, and S. Safari, Appl. Phys. Lett. **61**, 1537 (1992).

<sup>12</sup>M.-S. Chen, T.-B. Wu, and J.-M. Wu, Appl. Phys. Lett. **68**, 1430 (1996).